

Electrochemical synthesis, characterization and magnetic studies of Ni/TCNQ salts

Gregory Long ^a, Roger D. Willett ^{b,*}

^a Department of Chemistry, Minnesota State University, Mankato, MN 56002, USA

^b Department of Chemistry, Washington State University, Pullman, WA 99164, USA

Received 24 March 2000; accepted 28 June 2000

Abstract

Two new materials, Ni(TCNQ) and Ni₃(TCNQ)₂, have been obtained by an electroplating technique and characterized by SEM, XPS, vibrational spectroscopy, X-ray diffraction and magnetic techniques. The compound Ni(TCNQ), obtained at lower applied voltages, contains paramagnetic Ni(II) cations and diamagnetic TCNQ⁻² anions. In contrast, the material obtained at higher applied voltages, Ni₃(TCNQ)₂, contains diamagnetic Ni(II) cations and $S = 1/2$ TCNQ⁻³ anions. Thus, the higher oxidation states of the organic ligand have been stabilized by control of the applied electroplating voltage. Magnetic studies of polycrystalline samples of both compounds show the presence of dominant ferromagnetic interactions at higher temperatures, but antiferromagnetic interactions dominate at low temperatures. © 2001 Elsevier Science B.V. All rights reserved.

Keywords: Electrochemistry; Vibrational spectroscopy; X-ray diffraction; Magnetic studies; Ni/TCNQ solutions

1. Introduction

The development of present day experimental and theoretical condensed matter chemistry and physics is deeply indebted to magnetism and the magnetic behavior of many advanced materials [1].

Initially, compounds based on molecular and/or polymeric materials that display significant magnetic behavior were thought unlikely due to their relatively low spin densities. However, the discovery in the mid 1980s [2–4] of the transition metal–phthalocyanine magnets, all of which display significant magnetic transition temperatures in the range of liquid helium measurements, and the reports [5–8] in 1991 of transition metal–TCNE based polymeric magnets and of a Prussian Blue analog with transition temperatures above room temperature, have accelerated research efforts directed at the development and understanding of molecular/polymeric magnets.

In general, molecular-based magnets, which are usually composed of an inorganic component such a tran-

sition metal ion and an organic constituent such as a protonated amine, can be classified according to the orbitals in which the spins responsible for the magnetic behavior reside [9]. The organic moiety may be an active magnetic component of the material with its spin sites contributing to both the non-zero magnetic moment as well as any associated spin coupling. Alternatively, the organic moiety may be a passive component by only providing a means of positioning the spins, which reside solely on metal ions, so as to facilitate their coupling. As such, molecular based magnets are qualitatively distinct from conventional inorganic based magnets such as CrO₂.

During the past few decades, chemists and material scientists have been actively employing an interdisciplinary molecular engineering strategy, by coupling inorganic and organic techniques and synthetic methods, so as to achieve novel magnetic systems that undergo a spontaneous magnetic phase transition at a finite temperature [10–12].

In recent years there has been renewed interest in molecular magnets, due to the report of two systems which exhibited permanent moments at room temperature. Verdaguer et al. [8] used a systematic theoretical

* Corresponding author. Fax: +1-509-3358867.

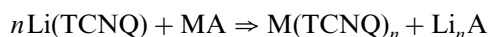
E-mail address: willett@mail.wsu.edu (R.D. Willett).

approach to design a series of Prussian blue analogs that have high values of Tc. This has spurred further studies of cyanide based systems [13–15]. In addition, electron transfer salts have become an aggressively studied class of low dimensional magnetic materials due, in part, to the recent discovery of the material $[V(\text{TCNE})_x]_y(\text{CH}_2\text{Cl}_2)$ which exhibits spontaneous magnetization at room temperature [16–18]. Although this material is pyrophoric and is difficult to characterize, it nonetheless represents a significant advance in the development of molecular magnets as a potential device for industrial applications.

In our efforts with new synthetic strategies for molecular magnets, we have decided to focus initially on the electron transfer-salts of the transition metal ions and the electron acceptor tetracyanocarbon ligand 7,7,8,8-tetracyanoquinodimethanide (TCNQ) [19]. Potember and coworkers [20–22] discovered that the material can switch from a high impedance to a low impedance material by applying an electric field across a M–TCNQ–M' (where M = Cu or Ag) device. In addition, this impedance change can also be induced by laser radiation [23–25]. Although other inorganic materials such as the chalcogenide semiconductors exhibit this behavior, the M–TCNQ–M' systems were the first hybrid organic–inorganic compound to do so. Although no device has been produced to date, this optical switching capability of Cu(TCNQ) suggests that the material may be hold potential applications as an optical data storage device [26–28].

Due to its demonstrated versatility as an electron acceptor molecule and its ability to form several stable radical species [29], and the ability of these reduced species to coordinate to a metal center as a σ -donor via one or more of its nitrile groups [30], TCNQ is a useful organic acceptor molecule that has yielded a wide variety of interesting molecular magnets [31].

The most common synthetic method for TCNQ based materials involves a metathesis reaction between an alkali metal salt of the TCNQ anion and a suitable salt, typically a halide, of a transition metal ion in acetonitrile [32–34].



In most cases, however, such preparative methods lead to materials that do not exhibit significant temperature dependent magnetic susceptibilities [35]. This is due, at least in part, to the tendency of the $S = 1/2$ TCNQ⁻¹ anion to dimerize into one-dimensional anti-ferromagnetic chains in the solid state [36] such that coupling between paramagnetic metal ions is minimized.

The questionable degree of purity that can be attributed to the very fine microcrystalline powders deposited from solutions can also have a pronounced effect on their electrical and magnetic properties [37]. A

hydrolysis product of TCNQ, the anion of α,α -dicyano-*p*-toluoylcyanide (DCTC⁻¹), in particular, is a common impurity in solution derived materials that can have pronounced effects on the bulk magnetic properties of metal–TCNQ salts [38] due to its $S = 0$ diamagnetic ground state.

In addition to the difficulty of preparing impurity-free materials, the solution metathesis methods have also been relatively unsuccessful in their ability to control morphologies and stoichiometries of metal–TCNQ thin-films or in yielding stable materials containing higher oxidation states of the TCNQ anion [39]. The lowest oxidation state, TCNQ⁻³, is particularly difficult to stabilize in solution prepared materials.

In this work, a unique electrochemical method of preparation similar to that outlined by Shields [40] has been employed to synthesize Ni(II) salts of TCNQ and to characterize their magnetic properties. As will be shown, this method of preparation offers several distinct advantages over traditional solution methods, such as the minimization of impurities, improved control over product stoichiometry, as well as the ability to produce stable compounds of the higher TCNQ anionic oxidation states.

After this project was underway, it was learned the Professor Kim Dunbar was investigating the transition metal–TCNQ species obtained by solution methods. For M = Ni(II), a Ni(TCNQ)₂ salt containing the TCNQ⁻¹ anion is obtained [41].

The next section describes the synthetic method as well as the battery of investigative methods used to characterize the materials produced via the electrochemical technique, while the subsequent sections document the results and conclusions. In particular, we show that the electrochemical technique can be used to control the oxidation state of the TCNQ species.

2. The synthetic method and characterization techniques

In this work, an electrochemical method of preparation similar to that outlined by Shields [40] has been employed to produce both bulk and thin film metal–TCNQ compounds. As will be shown, this method of preparation appears to offer several distinct advantages over traditional solution methods [42], including minimization of impurities and enhanced control over both product stoichiometry and thin-film deposition morphologies.

2.1. Experimental

The electrochemical cell used for the synthesis of all materials presented in this work consists of a two electrode system as shown schematically in Fig. 1. The cell was powered by a McKee–Pherson Electronics Inc.

d.c.-stabilized potentiostat and, in each case, the intrinsic impedance ($M\Omega$) of the cell assured that the current was < 1 mA. The distance between the electrodes was kept constant at 1 cm. The effects of varying voltage will be discussed in a subsequent section.

2.2. Reagents

The solvent used was Aldrich HPLC spectroscopic grade degassed acetonitrile. TCNQ was also from Aldrich and was sublimed twice under vacuum at 180°C and subsequently re-crystallized twice from spectroscopic grade degassed acetonitrile prior to use. The same batch of purified TCNQ, which was stored in a dessicator, was used for all of the materials synthesized in this work.

The substrate electrodes consisted of platinum foil purchased from Aldrich at 99.999% purity. The foil was cut to the desired size and cleaned with a 1:1 HNO_3 acid: H_2O solution, dried at 150°C overnight and cooled in a dessicator prior to use.

The nickel source electrodes were also purchased from Aldrich as foils at 99.999% purity. As before, each was cut to the desired size and cleaned with a 1:1 HNO_3 acid: H_2O solution, dried at 150°C overnight and cooled in a dessicator prior to use.

2.3. Method

In all cases, 50 ml of the HPLC grade acetonitrile was transferred to the reaction cell and purged with dry helium gas via the purge needles illustrated in Fig. 1 for 15 min prior to the introduction of the TCNQ so as to minimize the formation of the hydrolysis product DCTC. Re-crystallized TCNQ (0.255 g) was then added to the cell so as to form a 0.05 M solution (solution is nearly saturated). The solution was then purged again with dry helium for 10 min. Upon introduction of the source and substrate electrode assembly, the cell was again purged with helium and then biased to the desired d.c. voltage. Within 15–120 min, depending upon source material and cell bias, the desired product material began precipitating out of solution at the surface of the cathodic electrode. The cell was allowed to run (30 min to 3 days depending on source and bias) until the surface coverage of the cathodic platinum foil was deemed sufficient by eye so as to provide adequate yield of product. Upon completion of the product deposition, the substrate electrode was removed from the assembly and the product was washed with several volumes of degassed acetonitrile and allowed to dry in a dessicator at room temperature prior to subsequent analysis.

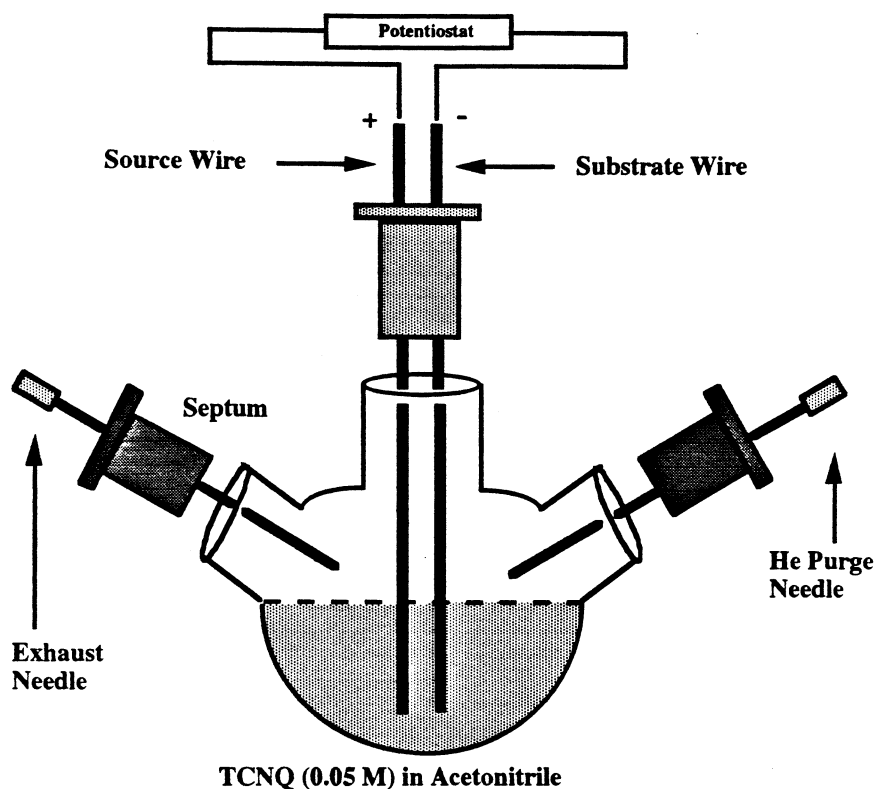


Fig. 1. A schematic illustration of the electrochemical cell used to synthesize metal–TCNQ compounds from 0.05 M acetonitrile solution. The cell atmosphere consisted of dry helium gas during the synthesis.

Table 1
Analytical data for electrochemically synthesized Ni–TCNQ complexes

Compound	Anal. Found (Calc.) (%)			
	C	H	N	Ni
Ni(TCNQ) (1)	54.7 (54.8)	1.5 (1.5)	21.3 (21.3)	22.5 (22.4)
Ni ₃ (TCNQ) ₂ (2)	49.3 (49.3)	1.4 (1.4)	19.2 (19.0)	30.1 (30.3)

The low voltage product Ni(TCNQ) (1) and the high voltage product Ni₃(TCNQ)₂ (2), were synthesized at a constant 5 and 10 d.c. V applied cell bias, respectively, for a period of 72 h. In both cases the size of the platinum cathode was 3.0 × 0.30 cm. Analytical data for these materials are given in Table 1.

2.4. Scanning electron microscopy and energy dispersive X-ray analysis

The SEM and EDX [43] analyses for all materials produced in this work were conducted using a JEOL JSM 6400 scanning electron microscope (SEM) fitted with a LINK Analytical Si(Li) EDX detection system. The EDX spectra for all of the washed and dried M(TCN)Q products were acquired prior to removal from the platinum substrates at an SEM accelerating voltage of 20 kV and a working stage distance of 8 cm. The platinum electrode was in all cases anchored to the brass SEM stage with both conductive graphite tape and a metallic grounding screw. The SEM micrographs of the materials were acquired at magnifications and accelerating voltages as specified on an individual basis. Due to the absence of significant charging effects [44], none of the materials analyzed were sputter coated with an Au film prior to analysis.

2.5. Infrared spectroscopy

The washed and dried product materials were removed from the surface of the platinum cathode using a Kel-F spatula. A small sample of the materials were then homogenized, using an agate mortar and pestle, with KCl which had been dried at 200°C overnight and then cooled in a dessicator prior to use. The diffuse reflectance IR spectra of the materials were acquired with an IBM Instruments IR-98 Fourier transform infrared spectrometer with a TGS detector. All of the spectra, which were background corrected and are reported in units of absorbance, were acquired at 4 cm⁻¹ resolution (2 cm⁻¹ per data point) with 512 scans coadded.

2.6. X-ray photoelectron spectroscopy

XPS spectra for all of the materials reported in this work were determined using a Kratos Analytical Axis 165 electron spectrometer using Mg–K_α X-rays. All of the samples, which had been isolated from the platinum cathode using a Kel-F spatula and were washed and dried as specified earlier, were analyzed as powders pressed into clean indium foil. No compensation for sample charging effects was necessary. The metal 2p_{3/2} binding energies, nitrogen 1(s) binding energies, Auger line energies and Auger parameter energies are the average of at least five replicate measurements with the confidence limits taken as the standard deviations of the sample set.

2.7. Powder X-ray diffraction

No samples of the electrochemically synthesized transition metal complexes of TCNQ suitable for single crystal X-ray diffraction analysis have been produced. However, in order to explore relative differences in their structures, particularly as a function of applied cell voltage, the materials described in this work have been analyzed via powder X-ray diffraction.

The X-ray powder patterns were collected with a Siemens D501 diffractometer using copper K_α radiation. The samples were removed from the platinum electrode, washed and dried as discussed earlier, and homogenized with an agate mortar and pestle prior to analysis. Indexing of the patterns was completed using the Appleman [45] software in all cases.

2.8. Magnetic susceptibility

The magnetic susceptibility for powder samples all of the M(TCNQ) compounds reported in this work were determined from 4.4 K using a Lakeshore 7000 a.c. susceptometer. All of the data were background corrected between 4.4 and 300 K using a delrin sample container. Corrections for diamagnetic behavior were estimated from Pascal's constants [46].

3. Results and discussion

The EDX spectrum exhibits the characteristic K_α, K_β and average L_{αβ} X-rays of nickel at 7.5, 8.3 and 0.85 eV, respectively. No other impurities to which EDX is sensitive, such as metals or non-metallic elements with Z > 10, are present at a detectable level. The EDX spectrum of compound 2 is identical to that of compound 1 and again shows no evidence of contamination.

3.1. Structural studies

Powder X-ray diffraction data for compounds **1** and **2**, presented in Section 2, are also presented in Figs. 2

and 3, respectively. Both materials are polycrystalline in nature and exhibit different powder patterns thus suggesting the electrochemical method of preparation may give rise to structural variations in the nickel products

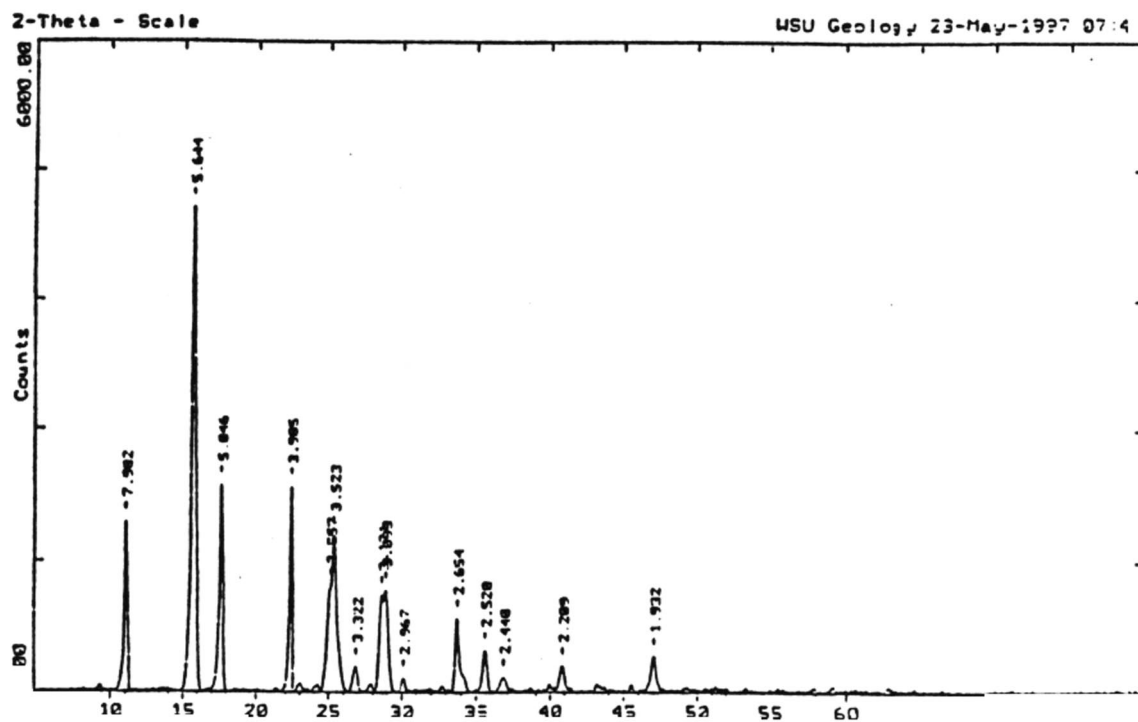


Fig. 2. X-ray diffraction powder pattern of **1**.

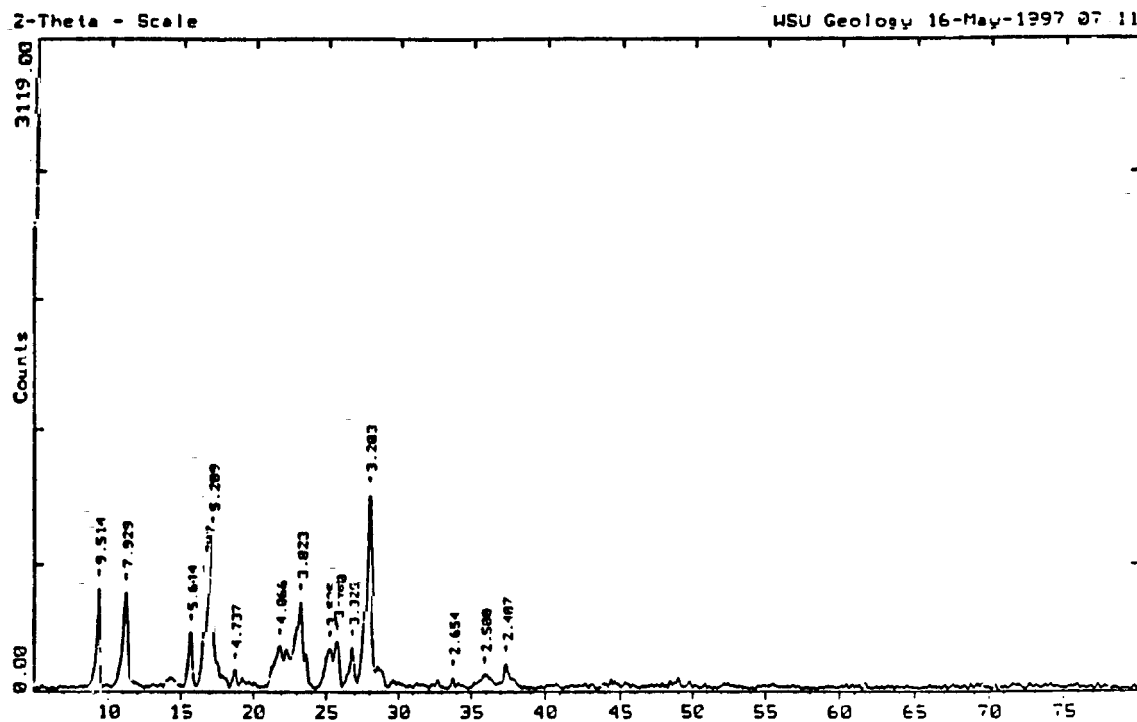


Fig. 3. X-ray diffraction powder pattern of **2**.

Table 2
Vibrational peak positions (cm^{-1}) for $\delta(\text{C-H})$ IR bands for TCNQ, TCNQ anions and DCTC salts

TCNQ	TCNQ ⁻¹	TCNQ ⁻²	TCNQ ⁻³	Cu(DCTC)	Ag(DCTC)	Assignment
859	802	822	812	834	835	b_{3u}
	823		819			b_{3u}
			822			b_{3u}
		1046				b_{2g}

as a function of applied cell voltage. Indexing of the major reflections present in the powder pattern of compound **1** suggest a cubic lattice with cell dimensions of 10.78(2) Å. When additional reflections, which are also shown in Fig. 2, are included in the indexing routine, no reliable solution is possible. These additional reflections, which do not correspond to known reflections of crystalline TCNQ [47], are, although relatively weak, reproducible and are above the estimated background noise present in the diffractometer. They are therefore considered to be real and suggest that the true structure has a lower symmetry structure.

The major reflections present in the powder pattern of compound **2**, as shown in Fig. 3, can be indexed on a tetragonal cell with dimensions $a = 10.898(12)$ and $c = 3.008(29)$ Å. However, as in the case of the low voltage product, when additional reflections, which again are reproducible and above background, are included in the indexing routine no reliable solution is found. These additional reflections suggest a distortion of the lattice to one of symmetry lower than tetragonal.

3.2. Spectroscopic studies

The number and frequencies of the IR bands of TCNQ are highly indicative of its oxidation state and coordinate status [48–53]. In addition, solution synthesized polycrystalline samples of copper and silver salts of DCTC have been studied via IR spectroscopy [54]. As is shown in Table 2, the IR spectra of the copper and silver salts of DCTC, which are relatively independent of ion environment, are distinctively different from those of TCNQ in the $\delta(\text{C-H})$ IR region and can thus be used as a probe for the presence of this hydrolysis product. Further studies of solution prepared copper salts of TCNQ deposited on the surface of copper foil [55] suggest that an impurity level of as little as 3% of DCTC by mass is detectable by infrared spectroscopy for metal–TCNQ salts in the solid state.

The diffuse reflectance infrared spectra in the $\delta(\text{C-H})$ region for compound **1** are given in Figs. 4 and 5. As is shown, compound **1** gives a single band in the $\delta(\text{C-H})$ regions at 815 and 1050 cm^{-1} which is indicative of the TCNQ⁻² anion [48,51]. The slight shift in the frequencies of these two bands, relative to observed stretches in alkali metal salts of TCNQ, is on the order of ca. 4

cm^{-1} and is consistent with other nickel salts of TCNQ⁻² prepared by solution methods [56]. The characteristic b_{3g} band of DCTC⁻¹ at 835 cm^{-1} is not evident in the $\delta(\text{C-H})$ spectra of compound **1**, suggesting that no significant contamination from the hydrolysis product is present. Furthermore, the lack of absorption maxima in the $\delta(\text{C-H})$ region 850–880 cm^{-1} suggest that no neutral TCNQ⁰ is present in the material.

The IR spectrum of compound **2** in the $\delta(\text{C-H})$ region is shown in Fig. 6. For the high voltage product, two strong bands are present at 809 and 828 cm^{-1} , which are consistent with stretches observed for the TCNQ⁻³ anion in the solid state [48,57]. As with compound **1**, no evidence of either the hydrolysis product DCTC nor neutral TCNQ⁰ is detectable in the spectrum.

The $\nu(\text{C-N})$ bands for compounds **1** and **2** are shown in Figs. 7 and 8, respectively. This region of the IR spectra can yield information regarding the coordinate status of the TCNQ anion within the solid state material. In uncomplexed TCNQ⁻² and TCNQ⁻³ only two

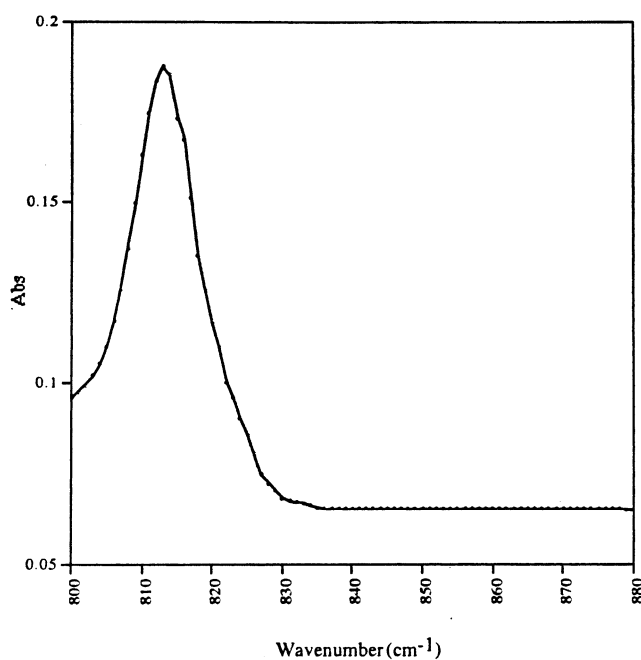


Fig. 4. $\delta(\text{C-H})$ infrared bands in the 800–880 cm^{-1} region for **1**.

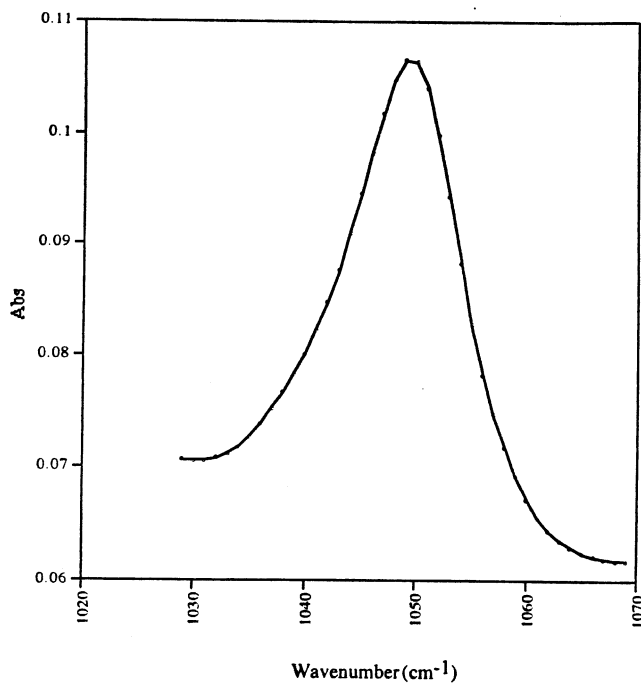


Fig. 5. $\delta(\text{C-H})$ infrared bands in the $1030\text{--}1060\text{ cm}^{-1}$ region for **1**.

$\nu(\text{C-N})$ stretches in the $2000\text{--}2300\text{ cm}^{-1}$ region are expected and found [58]. The occurrence of multiple $\nu(\text{C-N})$ bands, as observed in both of these compounds, has been attributed to a reduction in symmetry of the TCNQ anion caused by an interaction between

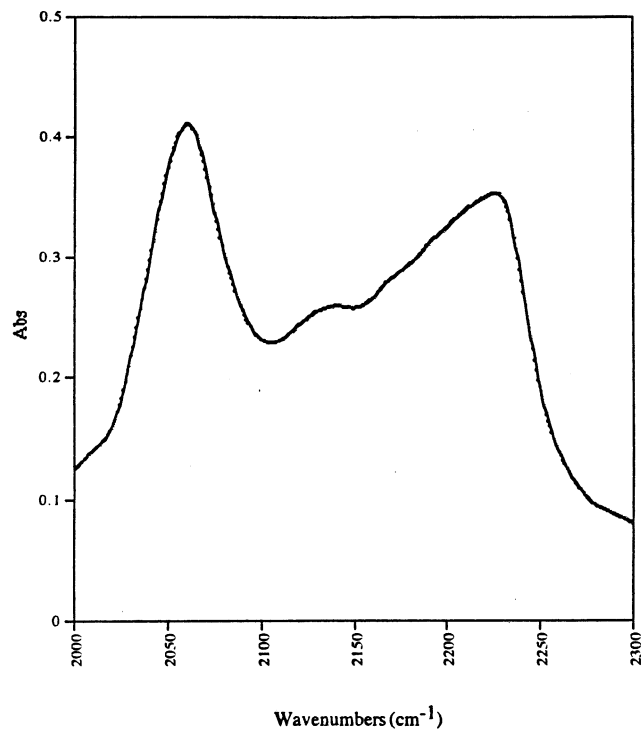


Fig. 7. $\nu(\text{C-N})$ infrared bands for **1**.

the highly polarizing positively charged metal center and the cyano groups of the TCNQ anions [59]. Such interactions have been observed in the compound

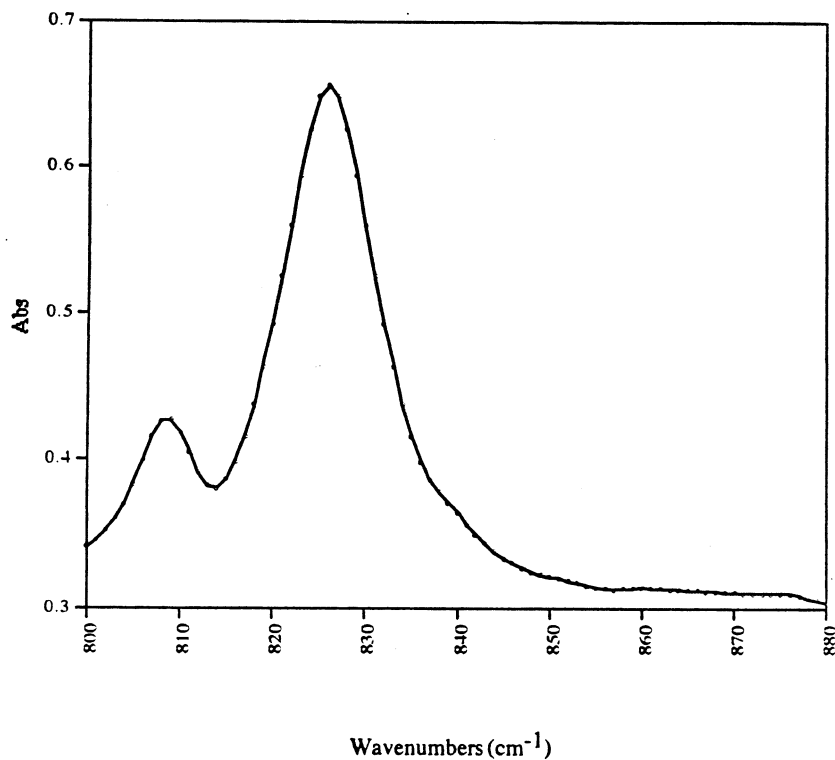


Fig. 6. $\delta(\text{C-H})$ infrared bands in the $800\text{--}880\text{ cm}^{-1}$ region for **2**.

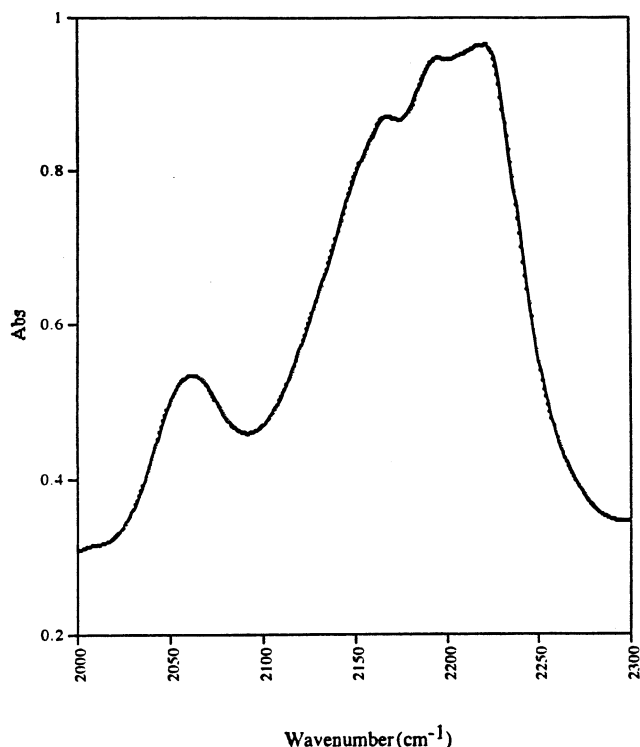


Fig. 8. $\nu(\text{C-N})$ infrared bands for **2**.

$(\text{C}_5\text{H}_2)_2\text{VBr-TCNE}$ [60] and in the silver cyanocarbon derivatives $\text{AgC}(\text{CN})_2\text{NO}$ [61] and $\text{AgC}(\text{CN})_2\text{NO}_2$ [62].

Studies of transition metal derivatives of TCNQ by Azcando et al. [63] suggest that the splitting of the $\nu(\text{C-N})$ bands of TCNQ anions into three or more bands in the solid state is a result of direct alpha coordination of the anions to the metal center through the negative charge density of the cyano groups, as opposed to coordination of the metal ion to the TCNQ anions through the π -electron density of the ring. In addition, studies of metal-TCNQ derivatives by Cornelisson suggest that the splitting of these bands is often accompanied by a frequency shift of the $\nu(\text{C-N})$ bands to slightly higher energies relative to bands observed in uncoordinated ligands [64]. Comparison of the $\nu(\text{C-N})$ band splitting observed in compounds **1** and **2** with that observed by Azcando et al. suggest that the TCNQ anions in both electrochemically synthesized materials may be coordinated directly to the metal center through one or more of the terminating cyano groups.

X-ray photoelectron spectroscopic (XPS) measurements for the nickel and nitrogen atoms of compounds **1** and **2** are shown in Figs. 9 and 10, and were obtained with a magnesium K_{α} X-ray source. In the past several decades, a plethora of studies of transition metal compounds have demonstrated that experimentally measured binding energies of metal ion core electrons often differ significantly between materials where the metal ions are either exposed to different chemical environments in the solid state or are present in different

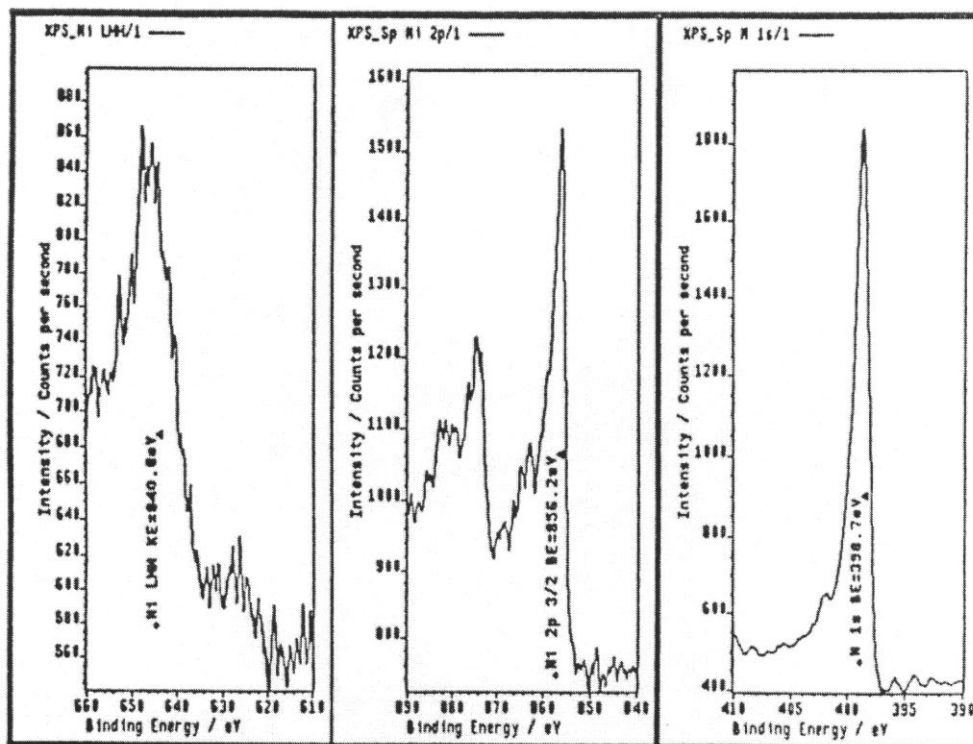


Fig. 9. Nickel and nitrogen XPS spectra for compound **1**.

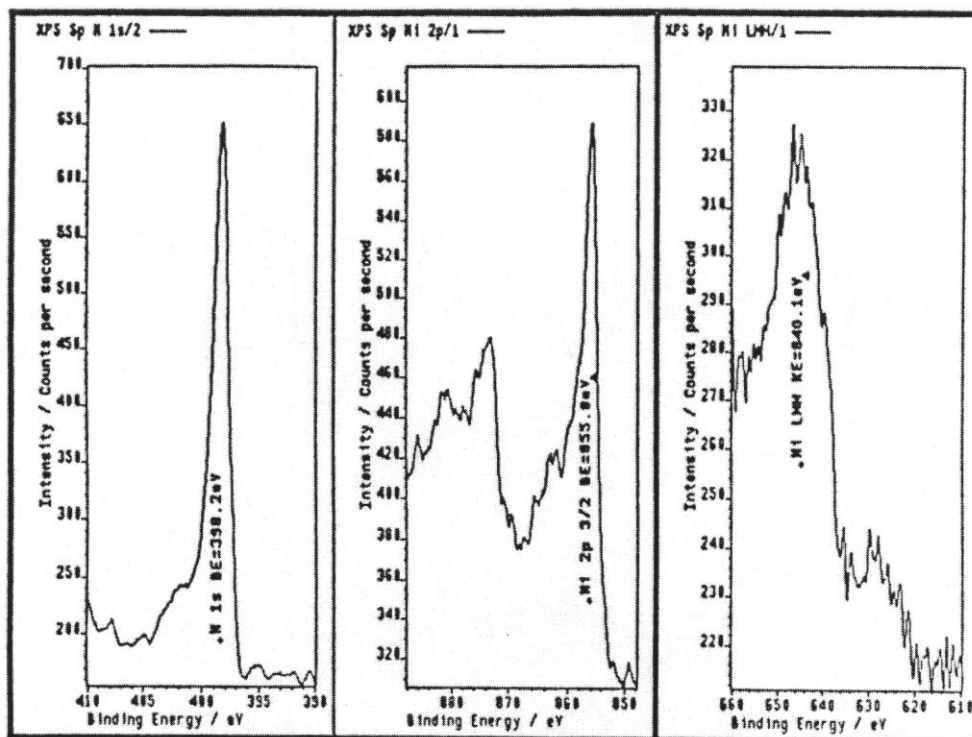


Fig. 10. Nickel and nitrogen XPS spectra for compound 2.

oxidation states [65–69]. Measured differences in core electron binding energies for a variety of different transition metal materials have been tabulated [70] and are often used as a probe of the ion environments and charge states.

The most reliable, and most common method of determining metal ion oxidation states using electron spectroscopy is by the determination of the Auger parameter [71], which is defined by Wagner [72] as the sum of the kinetic energy of the most intense Auger line and the binding energy of the most intense photoelectron line. Similar to the XPS core electron binding energies, the Auger parameters of transition metal compounds are also extensively tabulated [73]. The Auger parameters and binding energies of the XPS $2p_{3/2}$ lines differ significantly as the chemical environment and oxidation state of the copper ion changes. In this work, the oxidation state of the metal ion in the $M(\text{TCNQ})$ products were estimated by comparison of tabulated Auger parameters and XPS $2p_{3/2}$ line energies of similar materials with experimentally determined values.

The measured nickel $2p_{3/2}$ binding energy for compound 1, 856.3 eV is consistent with a $3d^8$ Ni(II) ion which may be coordinated to a nucleophilic moiety such as a cyanide ligand or an organic amine [74]. The kinetic energy of the LMM_2 Auger transition, measured at 840.9 eV, yields a calculated Auger parameter of 1697.2 eV. This is further indicative of a +2 oxidation

state for the nickel ion and also suggests that the metal ion is coordinated to a nitrogen containing ligand such as an organo-cyanide [75]. The binding energy of the measured nitrogen 1s XPS transition at 398.3 eV is in further agreement with literature values of reduced organic amines, cyanide in particular, coordinated to metal atoms in the solid state [76]. No evidence of other nickel transitions appear present in the spectrum, which suggests that the material does not contain oxidation states of the metal atom other than the +2 state.

The nickel $2p_{3/2}$ binding energy for compound 2, at 855.8 eV, is strongly indicative of a Ni(II) ion coordinated directly to one or more cyanide ligands such as in $\text{K}_2\text{Ni}(\text{CN})_4$ [77]. The slight reduction of the $2p_{3/2}$ binding energy of this line in the XPS spectra of compound 2, relative to compound 1, is predictable due to the decrease in electronegativity of the TCNQ anion with increasing charge. The Auger parameter calculated for this material, based on the measured kinetic energy of the LMM_2 Auger transition of the nickel atom is 1695.9 eV, and is further consistent with values observed for nickel atoms in the +2 oxidation state coordinated to cyanide ligands [77]. As seen in compound 1, the measured binding energy of the nitrogen 1s XPS line for compound 2, at 398.2 eV, is again in excellent agreement with values observed for Ni(II) compounds in which direct coordination of the cyanide ligand to the metal center is present [61]. Again, no evidence of

oxidation states other than +2 for the metal is present in the spectrum.

3.3. Magnetic susceptibility and EPR studies

The magnetic susceptibility of compounds **1** and **2** were measured from 4.4 up to ca. 200 K. Both materials were studied at a frequency of 375 Hz and an a.c. excitation field of 0.4 Oe. EPR measurements on powdered samples of both materials were taken with a Bruker EP300 X-band spectrometer at a microwave frequency of 9.3 GHz at room temperature. The average g values obtained from these measurements were used to fit the susceptibility data. Diamagnetic corrections for both materials were estimated from Pascal's constants.

The magnetic susceptibility data of compound **1** and **2**, shown in Figs. 11 and 12, respectively, show evidence of two types of magnetic interaction: a dominant ferromagnetic exchange at high temperature which causes

$\chi_M T$ to increase with decreasing temperatures and a weaker antiferromagnetic exchange that becomes important at lower temperatures which tends to align the resultant moments antiparallel. Compound **1** and **2** show maxima in $\chi_M T$ at $T_c = 28.3$ and 8.6 K, respectively.

The deviation from Curie behavior of the data at low temperatures present in both χ_M^{-1} plots is characteristic of systems which are not pure Curie magnets and suggests the presence of magnetic coupling between paramagnetic moieties, significant zero-field splittings or a combination of the two, as is often the case with nickel compounds [78]. At higher temperatures, where the data are expected to follow Curie behavior, linear least-squares regression of the data for compound **1** suggests a Curie constant of $1.19 \text{ emu K mol}^{-1}$ and a Curie–Weiss constant of 22.6 K. These values are consistent with the reported stoichiometry of Ni(TCNQ) which contains one paramagnetic $S = 1 \text{ } 3d^8$ Ni(II) ion and one $S = 0$ diamagnetic TCNQ species

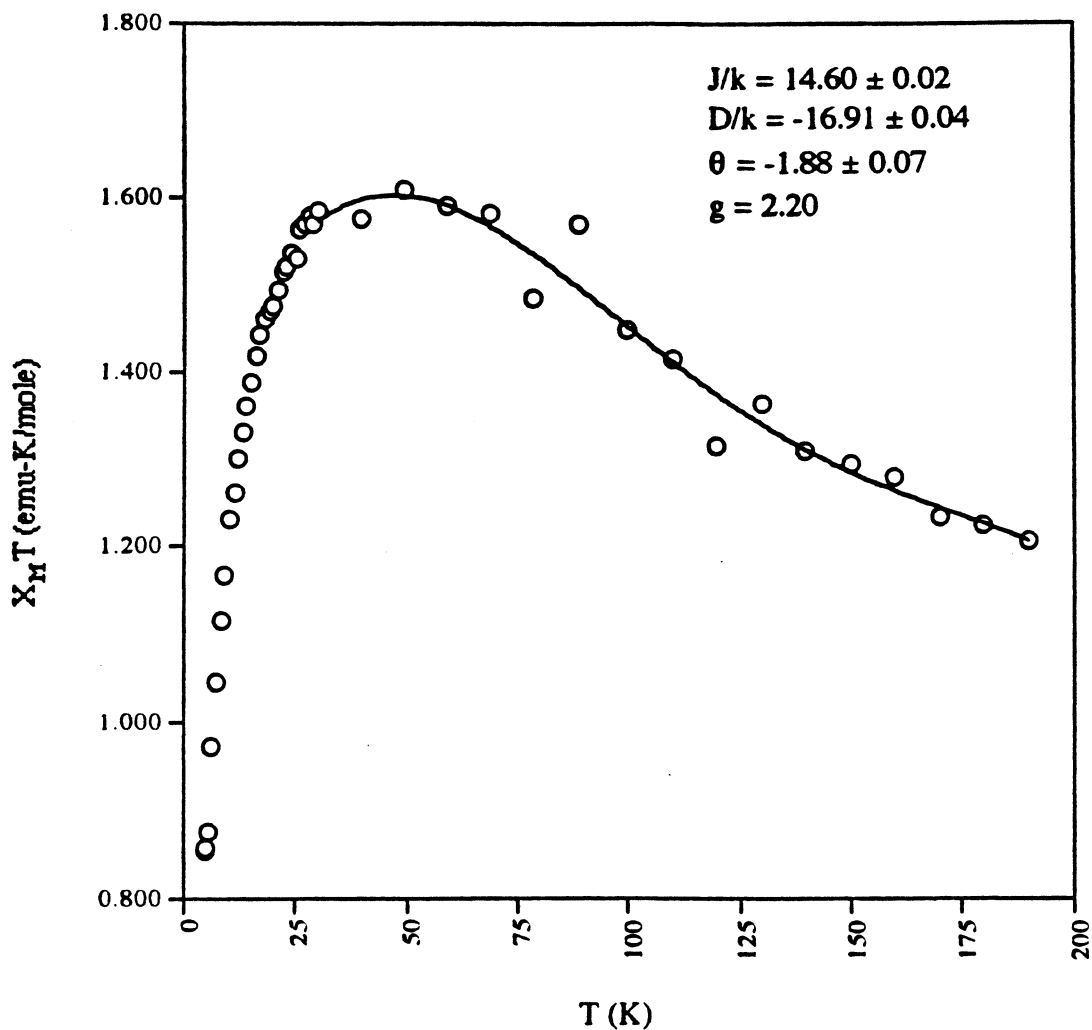


Fig. 11. Plot of $\chi_M T$ versus T for **1**. (Experimental data, \circ ; best fit, —).

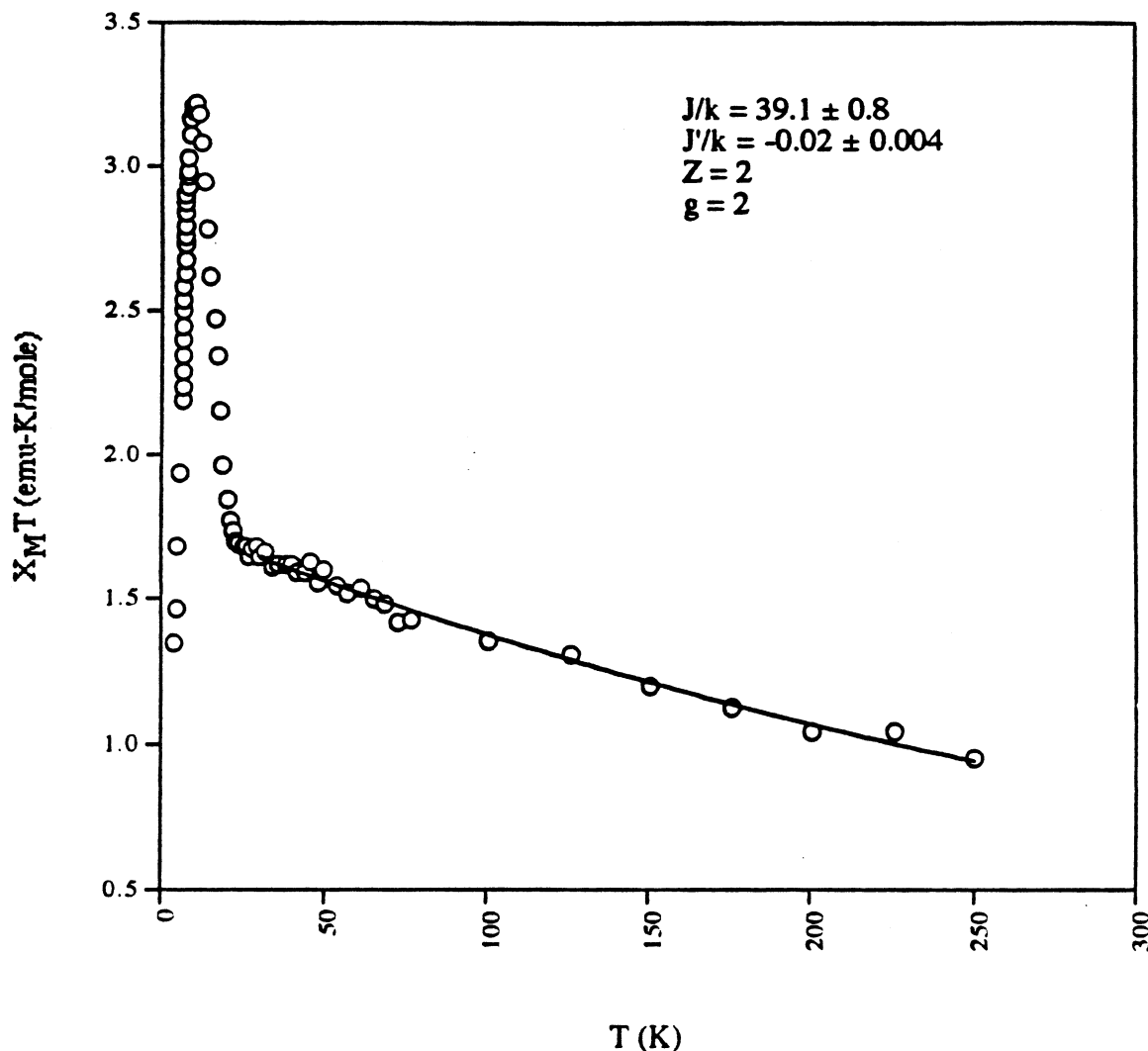


Fig. 12. Plot of $\chi_M T$ versus T for **2**. (Experimental data, \circ ; best fit, —).

per mole of compound. The positive value of the Curie–Weiss constant suggests the presence of predominant ferromagnetic behavior at high temperatures [79]. The value of the Curie constant obtained from the regression, $1.19 \text{ emu K mol}^{-1}$, is also consistent with a high temperature extrapolation of the $\chi_M T$ data in Fig. 11.

The EPR spectrum of compound **1** at room temperature consisted of a single symmetric broad line centered at $g = 2.20$ with peak-to-peak line width of ca. 600 Oe as expected for an $S = 1$ Ni(II) ion. The diamagnetic TCNQ $^{-2}$ is not expected to contribute to the EPR spectrum of the material, and no evidence of a sharp $g = 2.00$ signal due to a TCNQ $^{-1}$ or TCNQ $^{-3}$ species is present.

Linear regression of the high temperature Curie data for compound **2** yields a Curie constant of $0.8 \text{ emu K mol}^{-1}$ which is consistent with paramagnetic contributions only from two $S = 1/2$ TCNQ $^{-3}$ species per mole of material. The Curie–Weiss constant, calculated from

the fitting as 47.2 K, is positive as expected for ferromagnetic interactions.

The value of the Curie constant obtained from these calculations, which is consistent with the high temperature extrapolations of the data in Fig. 12, is interesting in that it is approximately an order of magnitude lower than expected if the contributions of three paramagnetic $S = 1$ Ni(II) ions per mole of material are considered. The diamagnetic behavior of the metal ions is expected, however, if the Ni(II) ions have a square-planar D_{4h} geometry as is known to occur with strong field ligands such as the cyanides [80]. Preliminary ab initio calculations conducted by Professor Ron Poshusta of Washington State University of TCNQ in the -1 , -2 and -3 oxidation states suggest an increase of electron density on the terminal cyano groups of TCNQ accompany a decrease in oxidation state. These calculations yield approximate an electron density value of -0.5 for each of the terminal nitrogen atoms in the TCNQ $^{-3}$ anion which may be sufficient to allow the

TCNQ anion to behave as a strong field ligand and thus force the nickel ions into a diamagnetic square planar geometry.

The qualitatively susceptibility data are indicative of low dimensional ferromagnetic coupling with weaker intersystem antiferromagnetic coupling. Thus, the susceptibility data was modeled with an appropriate low dimensional model. The susceptibility data above 30 K for compound **1** was fit to a high-temperature series expansion $S=1$ linear chain Heisenberg model [81] based on the Hamiltonian $H = -2J_{ij}S_i \cdot S_j$ that incorporates zero-field splitting terms for the nickel ions and mean-field correction terms which account for interchain interactions. Non-linear curve fitting of the data to this model, which gave an estimated goodness-of-fit parameter of 0.9998 [82] over the specified temperature range, suggests an intrachain coupling constant of $J/k = 14.6 \pm 0.02$ K, an interchain coupling constant of $J'/k = -1.88 \pm 0.04$ K, and a zero-field splitting constant of $D/k = -16.9 \pm 0.07$ K. The anisotropic g value, as measured from the EPR spectrum, was fixed at a value of $g = 2.20$ throughout the fitting routine.

The agreement between the calculated and observed susceptibility data and the values for the exchange constants derived from the fitting suggest that within this temperature range, the system exhibits predominant ferromagnetic interactions and that the material consists of a low dimensional magnetic lattice. The magnitudes of the intrachain coupling and zero-field splitting constants are in fairly good agreement with literature values reported for other linear chain Ni(II) compounds [83–86]. The sign of the interchain coupling constant $J'/k = -1.88 \pm 0.04$ K suggests that this interaction is antiferromagnetic in nature, which is expected from the low temperature behavior of the $\chi_M T$ data. The magnitude of this exchange constant is also within the range observed for other Ni(II) linear chain materials [83–86] and may suggest that the crystal lattice for the material is fairly small, as mentioned earlier, so as to allow for significant interchain contacts between paramagnetic moieties.

The EPR spectrum of compound **2** at room temperature shows a single sharp line centered at $g = 2.000$ with a peak-to-peak line width of ca. 50 Oe as expected for the $S = 1/2$ TCNQ⁻³ anions. The diamagnetic nickel ions are not expected to contribute to the EPR spectrum of the material, and no evidence of their contribution is present at detectable levels.

The susceptibility data above 35 K for compound **2** was fit to a $S = 1/2$ one-dimensional ferromagnetic chain Heisenberg model [87] based on the Hamiltonian $H = -2J_{ij}S_i \cdot S_j$ which incorporates a term for the number of equivalent nearest neighbor chains and a mean-field correction term for the interchain interactions. Non-linear curve fitting of the data to this model, which gave an estimated goodness-of-fit parameter of

0.9999 over the specified temperature range, suggest an intrachain coupling constant of $J/k = 39.1 \pm 0.8$ K and an interchain coupling constant of $J'/k = -0.02 \pm 0.004$ K. The best agreement between the experimental and calculated molar susceptibilities was given by fixing the value of the number of equivalent nearest neighbor chains parameter to 2. The anisotropic g value, as measured from the EPR spectrum, was fixed at a value of $g = 2.000$ throughout the fitting routine.

The magnitude and signs of the exchange constants derived from the fitting suggest that, as expected, ferromagnetic interactions predominate over this temperature range. The magnitude of the intrachain coupling constant, which stems from the paramagnetism of the TCNQ anions, is consistent with other Ni(II) derivatives which contain $S = 1/2$ TCNQ⁻¹ anions [88]. The sign and magnitude of the interchain coupling constant suggest that overall this interaction is antiferromagnetic in nature and is quite weak. However, due to the sharp increase in $\chi_M T$ at ca. 30 K may suggest the onset of long range order due to the presence of a second ferromagnetic pathway. Thus the nearly zero value derived for the interchain coupling may well be the consequence of nearly offsetting ferromagnetic and antiferromagnetic contributions. In the absence of single crystal structural data, the significance of the small negative value for the nearest neighbor chain parameter is difficult to assess. The aforementioned increase in $\chi_M T$ at 30 K and the onset of significant antiferromagnetic interactions at low temperatures suggest that the system may not be a true one-dimensional system at any temperature. Attempts to fit the susceptibility data, however, with several magnetic models that incorporate two-dimensional interactions, proved unsuccessful.

4. Conclusions

An electrochemical method has been used to successfully synthesize two new nickel complexes of TCNQ. Unlike solution methods, in which the oxidation state of the organic anion is difficult to control, the electrochemical method appears to readily yield stable compounds of various anion oxidation states as a function of applied cell bias. The elemental, EDX, IR and XPS data suggest that the stoichiometry of the products are Ni(TCNQ) and Ni₃(TCNQ)₂ when the reaction is carried out at 5 and 10 d.c V applied bias, respectively, with Ni(II) in both cases and TCNQ in the -2 and -3 oxidation states, respectively. This is in contrast to the Ni(TCNQ)₂ material obtained by Dunbar et al. from solution preparations, which contains the TCNQ⁻¹ anion. In addition, minimization of the hydrolysis product DCTC is possible when appropriate precautions are taken during the synthetic procedure.

The redox reaction of the TCNQ with the source metal that occurs in the cell is thought to take place via the following general reaction scheme:



where the reduction of the TCNQ takes place at the surface of the substrate electrode. The metal ions and the TCNQ anions then interact to form the insoluble complex which deposit at the surface of the substrate electrode.

Temperature dependent magnetic susceptibility measurements suggest that both materials exhibit low dimensional behavior with dominant ferromagnetic behavior at high temperatures with antiferromagnetic exchange interactions that dominate at low temperature. The magnetism in **1** appears to be due to spin-spin interaction between the paramagnetic Ni(II) ions mediated by diamagnetic TCNQ⁻² bridging ligands. For **2**, the TCNQ⁻³ ions act as strong field ligands, forcing the Ni(II) ions to form diamagnetic square planar complexes. Thus, the magnetism is due to interactions between the spin 1/2 ground states of the TCNQ⁻³ anions. The high voltage product Ni₃(TCNQ)₂ exhibits a sharp increase in $\chi_M T$ at ca. 30 K that may suggest the presence of additional antiferromagnetic interaction. Due to the observed splitting of the $\nu(\text{C-N})$ bands in the IR spectra of the materials, coordination of the TCNQ anions to the metal center is possible, but in the absence of single crystal structural data, it is difficult to determine the geometries of such exchange pathways. Assuming a tetragonal cell with a short axis of ca. 3 Å, it is possible that the material may consist of Ni-TCNQ chains that run parallel to the long axis of the unit cell. Stacking of these chains parallel to the short axis may then allow for short ligand-ligand contacts which are responsible for the observed magnetic behavior below 30 K. It is difficult, however, to envision the precise connectivity of the metal-TCNQ⁻³ species in this or any other unit cell so as to yield a square planar geometry for the nickel ions given the predicted stoichiometry. In order to provide such a geometry for each of the three nickel ions suggested by the molecular formula Ni₃(TCNQ)₂, a total of twelve coordinating species are required. Even assuming that the nickel ions are coordinated to the potentially bidentate dicyanomethylene groups of the TCNQ anions, the predicted stoichiometry only allows for eight such interactions. The presence of other coordinated species however, such as acetonitrile, is not supported by the

infrared or elemental analysis. Clearly, single crystalline samples are necessary to completely characterize this material in the solid state.

Recent studies [41] by Dunbar et al. at Michigan State University suggest that a similar magnetic behavior to that of compound **2** is seen in solution prepared nickel salts of TCNQ⁻¹. Although no single crystal structural data or magnetic modeling data are currently available for these materials, the similarities of the magnetic data suggest that the dramatic increase in the ferromagnetic interactions at 30 K is due to the onset of exchange via the $S = 1/2$ TCNQ anions in the lattice. Although TCNQ anions in the -1 and -3 oxidation state are known to exhibit both ferro and antiferromagnetic behavior via the ring π -electron density in the solid state [94-98] usually through the formation of dimeric units, the magnitude of the coupling is usually on the order of a few Kelvins and is thus unlikely to be solely responsible for the behavior seen in compound **2**.

References

- [1] National Research Council, Materials Science and Engineering for the 1990s, National Academy Press, Washington DC, 1989, p. 94.
- [2] J.S. Miller, P.J. Krusic, A.J. Epstein, W.M. Reiff, J.H. Zhang, *Mol. Cryst. Liq. Cryst.* 120 (1985) 27.
- [3] J.S. Miller, J.C. Calabrese, H. Rommelmann, S.R. Chittipeddi, J.H. Zhang, W.H. Reiff, A.J. Epstein, *J. Am. Chem. Soc.* 109 (1987) 769.
- [4] S. Chittipeddi, K.R. Cromack, J.S. Miller, A.J. Epstein, *Phys. Rev. Lett.* 58 (1987) 2695.
- [5] J.S. Miller, A.J. Epstein, The interconnection of chemical and electronic structure, in: Proceedings of the Nobel Symposium NS-81 on Conjugated Polymers and Related Materials, Oxford University Press, London, 1991, p. 461.
- [6] J.M. Manriquez, G.T. Yee, R.S. McLean, A.J. Epstein, J.S. Miller, *Science* 252 (1991) 1415.
- [7] J.S. Miller, G.T. Yee, J.M. Manriquez, A.J. Epstein, The interconnection of chemical and electronic structure, in: Proceedings of the Nobel Symposium NS-81 on Conjugated Polymers and Related Materials, Oxford University Press, London, 1991, p. 461.
- [8] T. Mallah, S. Thiebaut, M. Veraguer, P. Weillet, *Science* 262 (1993) 1554.
- [9] J.S. Miller, A.J. Epstein, in: P. Coronado, D. Delhaes, J.S. Gatteschi, D. Miller (Eds.), *Molecular Magnetism: From Molecular Assemblies to the Devices* (NATO ASI Series E), Kluwer, Dordrecht, 1995.
- [10] J.S. Miller, A.J. Epstein, *New Aspects of Organic Chemistry*, VCH, New York, 1989, p. 237.
- [11] A. Caneschi, D. Gatteschi, R. Sessoli, P. Rey, *Acc. Chem. Res.* 22 (1989) 392.
- [12] O. Kahn, Y. Journaux, *Inorganic Materials*, Wiley, New York, 1993, p. 59.
- [13] A.J. Epstein, in: J.S. Miller (Ed.), *Synthesis and Properties of Low Dimensional Materials*, New York Academy of Sciences, New York, 1978, p. 313.
- [14] W.R. Entley, G.S. Girolami, *Science* 268 (1995) 397.
- [15] S. Ferlay, T. Mallah, R. Ouahès, P. Veillet, M. Verdaguer, *Nature* 378 (1995) 701.

- [16] J.S. Miller, D.A. Dixon, J.C. Calabrese, C. Vazquez, P.J. Krusic, M.D. Ward, E. Wasserman, R.L. Harlow, *J. Am. Chem. Soc.* 112 (1990) 381.
- [17] P. Zhou, B.G. Morin, J.S. Miller, A.J. Epstein, *Phys. Rev. Sect. B* 48 (1993) 1325.
- [18] J.S. Miller, A.J. Epstein, *Chem. Eng. News* 73 (1995) 30.
- [19] L.R. Melby, R.J. Harder, W.R. Hertler, *J. Am. Chem. Soc.* 84 (1962) 3374.
- [20] R.S. Potember, T.O. Poehler, D.O. Cowan, P. Brant, *Chem. Scr.* 17 (1980) 219.
- [21] R.S. Potember, T.O. Poehler, D.O. Cowan, A. Rappa, A.N. Bloch, *Synth. Met.* 4 (1982) 371.
- [22] R.S. Potember, T.O. Poehler, R.C. Benson, R.C. Hoffman, E. Bourkoff, *Appl. Phys. Lett.* 42 (1983) 855.
- [23] W.M. Risen, E.I. Kamitsos, *Solid State Commun.* 45 (1983) 165.
- [24] W.M. Risen, E.I. Kamitsos, *J. Chem. Phys.* 79 (1983) 5808.
- [25] E.J. Kamistos, C.H. Tzinis, W.M. Risen, *Solid State Commun.* 42 (1982) 561.
- [26] R.C. Wheland, J.L. Gillson, *J. Am. Chem. Soc.* 98 (1976) 3916.
- [27] E.I. Kamistos, W.M. Risen, *Mol. Cryst. Liq. Cryst.* 134 (1986) 31.
- [28] S. Yamaguchi, C.A. Viands, R.S. Potember, *J. Vac. Sci. Technol.* B9 (1991) 1129.
- [29] S.E. Bell, J.S. Field, R.J. Haines, *Inorg. Chem.* 31 (1992) 3269.
- [30] B. Lanelli, C. Pecille, *J. Chem. Phys.* 52 (1970) 2375.
- [31] J.S. Miller, A.H. Reis, E. Gebert, J.J. Ritsko, W.R. Salaneck, T.W. Kovnat, R.P. Cape, *J. Am. Chem. Soc.* 101 (1979) 7111.
- [32] A.R. Siedle, G.A. Candela, T.F. Finnegan, *Inorg. Chim. Acta* 35 (1979) 125.
- [33] M.T. Azcondo, L. Ballester, L. Calderon, A. Gutierrez, F. Perpnan, *Polyhedron* 14 (1995) 2339.
- [34] J.S. Miller, A.J. Epstein, W.M. Reiff, *Chem. Rev.* 88 (1988) 201.
- [35] J.S. Miller, A.J. Epstein, *Prog. Inorg. Chem.* 20 (1974) 1.
- [36] D.S. Acker, W.R. Hertler, *J. Am. Chem. Soc.* 84 (1962) 3370.
- [37] K. Nakatani, T. Sakata, Tsubomura, *Bull. Chem. Soc. Jpn.* 48 (1975) 2205.
- [38] J. Gong, Y. Osada, *Appl. Phys. Lett.* 61 (1992) 2787.
- [39] (a) J.J. Hoagland, X.D. Wang, K.W. Hipps, *Chem. Mater.* 5 (1993) 54. (b) L. Ballester, M.C. Barral, R. Gutierrez, J.M. Jimenez-Aparicio, J.M. Martinez-Muyo, M.F. Perpnan, A. Monge, C. Ruiz-Valero, *J. Chem. Soc. Chem. Commun.* (1991) 1396.
- [40] L. Shields, *J. Chem. Soc. Faraday Trans. II* 81 (1985) 1.
- [41] K. Dunbar, private communication.
- [42] A.R. Siedle, *J. Am. Chem. Soc.* 97 (1975) 5931.
- [43] J.C. Russ, *Fundamentals of Energy Dispersive X-ray Analysis*, Butterworths, London, 1984.
- [44] C.E. Fiori, *A Procedure for Resolving Spectral Interferences in Energy Dispersive X-ray Spectrometry*, Special Technical Publication 604, National Bureau of Standards, US Department of Commerce, 1981, p. 238.
- [45] D. Appleman, USGS ACA Meeting, Cambridge, 1963.
- [46] O. Kahn, *Molecular Magnetism*, VCH, New York, 1993.
- [47] G.S. Long, unpublished results, Washington State University, 1995.
- [48] B. Lunelli, C. Pecille, *J. Chem. Phys.* 52 (1970) 2375.
- [49] S.E. Bell, J.S. Field, R.J. Haines, M. Moscherosch, W. Matheis, W. Kaim, *Inorg. Chem.* 31 (1992) 3269.
- [50] M.S. Khatkale, J.P. Devlin, *J. Chem. Phys.* 70 (1979) 1851.
- [51] J. Stanley, D. Smith, B. Latimer, J.P. Devlin, *J. Phys. Chem.* 70 (1966) 2011.
- [52] C. Pecile, R. Bozio, A. Girlando, *J. Chem. Soc. Faraday Trans.* 71 (1975) 1237.
- [53] S.E. Bell, J.S. Field, R.J. Haines, M. Moscherosch, W. Matheis, W. Kaim, *Inorg. Chem.* 31 (1992) 3269.
- [54] M. Harris, J.J. Hoagland, U. Mazur, K.W. Hipps, unpublished results.
- [55] J.J. Hoagland, PhD Thesis, Washington State University, 1992.
- [56] A.R. Siedle, G.A. Candela, *Inorg. Chem. Acta* 35 (1979) 125.
- [57] M.S. Khatkale, J.P. Devlin, *J. Chem. Phys.* 70 (1979) 1851.
- [58] R.G. Kepler, *J. Chem. Phys.* 39 (1963) 3528.
- [59] A. Bieber, J. Andre, *J. Chem. Phys.* 5 (1974) 166.
- [60] R.P. Shibevea, L.O. Atovmyan, L.P. Rozenberg, *Chem. Commun.* (1969) 649.
- [61] Y.M. Chow, D. Britton, *Acta Crystallogr., Sect. B* 30 (1974) 1117.
- [62] Y.M. Chow, D. Britton, *Acta Crystallogr., Sect. B* 30 (1974) 147.
- [63] M.T. Azcondo, B. Loreto, L. Calderon, A. Gutierrez, M.F. Perpnan, *Polyhedron* 14 (1995) 2339.
- [64] J.P. Cornelissen, J.H. van Diemen, L.R. Groeneveld, J.G. Haasnoot, A.L. Spek, J. Reedijk, *Inorg. Chem.* 31 (1992) 198.
- [65] G.J. Leigh, J. Bremser, *J. Chem. Soc. Dalton Trans.* (1972) 1216.
- [66] W.M. Riggs, *Anal. Chem.* 44 (1972) 830.
- [67] S.O. Grim, L.J. Matienzo, *J. Am. Chem. Soc.* 94 (1972) 5116.
- [68] P. Finn, Jolly, *Inorg. Chem.* 11 (1972) 1434.
- [69] L.J. Matienzo, W.E. Swartz, S.O. Grim, *Inorg. Nucl. Chem. Lett.* 8 (1972) 1085.
- [70] D. Briggs, M.P. Seah, *Practical Surface Analysis*, Wiley, New York, 1983.
- [71] C.D. Wagner, *Faraday Discuss. Chem. Soc.* 60 (1975) 291.
- [72] C.D. Wagner, H.L. Gale, R.H. Raymond, *Anal. Chem.* 51 (1979) 466.
- [73] D. Briggs, M.P. Seah, *Practical Surface Analysis*, Wiley, New York, 1983 Appendix 4.
- [74] S.O. Grim, L.J. Matienzo, W.E. Swartz, *J. Am. Chem. Soc.* 94 (1972) 5116.
- [75] L.O. Pont, A.R. Siedle, *Inorg. Chem.* 13 (1974) 483.
- [76] J.F. Weiker, L.R. Melby, R.E. Benson, *J. Am. Chem. Soc.* 86 (1964) 4329.
- [77] C.D. Wagner, L.H. Gale, R.H. Raymond, *Anal. Chem.* 51 (1979) 466.
- [78] R.L. Carlin, *Magnetochemistry*, Springer-Verlag, New York, 1986.
- [79] C. O'Conner, *Inorg. Chem.* 29 (1982) 203.
- [80] A.F. Cotton, *Advanced Inorganic Chemistry*, Wiley, New York, 1988.
- [81] M.E. Fisher, *Am. J. Phys.* 32 (1964) 343.
- [82] J. Kuo, *Transforms and Curve Fitting*, Wiley, New York, 1982.
- [83] N. Achiwa, *J. Phys. Soc. Jpn.* 27 (1969) 561.
- [84] C. Dupas, J. Renard, *J. Chem. Phys.* 61 (1974) 3871.
- [85] J.F. Acherman, G.M. Cole, S.L. Holt, *Inorg. Chem. Acta* 8 (1974) 323.
- [86] A. Stebler, H.U. Gudel, A. Furrer, J.K. Kjems, *Inorg. Chem.* 21 (1980) 380.
- [87] J.S. Miller, A.J. Epstein, *Angew. Chem., Int. Ed. Engl.* 33 (1994) 385.
- [88] H. Wang, Y. Chen, J. Li, *Inorg. Chem. Acta* 148 (1988) 261.